doi:10.1093/brain/awz176 BRAIN 2019: 142; 2402–2416 | 2402

BRAIN
A JOURNAL OF NEUROLOGY

# Vector-mediated L-3,4-dihydroxyphenylalanine delivery reverses motor impairments in a primate model of Parkinson's disease

**Carl Rosenblad,[1,2] Qin Li,[3] Elsa Y. Pioli,[3] Sandra Dovero,[4,5] André SLM Antunes,[6] Leticia Agúndez,[6] Martino Bardelli,[6] R. Michael Linden,[6] Els Henckaerts,[6] Anders Björklund,[2] Erwan Bezard[3,4,5] and Tomas Björklund[2,7]**

Ever since its introduction 40 years ago L-3,4-dihydroxyphenylalanine (L-DOPA) therapy has retained its role as the leading standard medication for patients with Parkinson's disease. With time, however, the shortcomings of oral L-DOPA treatment have become apparent, particularly the motor fluctuations and troublesome dyskinetic side effects. These side effects, which are caused by the excessive swings in striatal dopamine caused by intermittent oral delivery, can be avoided by delivering L-DOPA in a more continuous manner. Local gene delivery of the L-DOPA synthesizing enzymes, tyrosine hydroxylase and guanosine-tri-phosphate-cyclohydrolase-1, offers a new approach to a more refined dopaminergic therapy where L-DOPA is delivered continuously at the site where it is needed i.e. the striatum. In this study we have explored the therapeutic efficacy of adeno-associated viral vector-mediated L-DOPA delivery to the putamen in 1-methyl-4-phenyl-1,2,3,6-tetrahydropyridine-treated rhesus monkeys, the standard non-human primate model of Parkinson's disease. Viral vector delivery of the two enzymes, tyrosine hydroxylase and guanosine-5'-tri-phosphate-cyclohydrolase-1, bilaterally into the dopamine-depleted putamen, induced a significant, dose-dependent improvement of motor behaviour up to a level identical to that obtained with the optimal dose of peripheral L-DOPA. Importantly, this improvement in motor function was obtained without any adverse dyskinetic effects. These results provide proof-of-principle for continuous vector-mediated L-DOPA synthesis as a novel therapeutic strategy for Parkinson's disease. The constant, local supply of L-DOPA obtained with this approach holds promise as an efficient one-time treatment that can provide long-lasting clinical improvement and at the same time prevent the appearance of motor fluctuations and dyskinetic side effects associated with standard oral dopaminergic medication.

1 Division of Neurology, Department of Clinical Sciences, Lund University, Skane University Hospital, 221 84 Lund, Sweden
2 Wallenberg Neuroscience Center, Department of Experimental Medical Science, Lund University, 22184 Lund, Sweden
3 Motac Neuroscience, Manchester, UK
4 Université de Bordeaux, Institut des Maladies Neurodégénératives, Bordeaux, France
5 Centre National de la Recherche Scientifique Unité Mixte de Recherche 5293, Institut des Maladies Neurodégénératives, Bordeaux, France
6 Department of Infectious Diseases, School of Immunology and Microbial Sciences, King's College London, London, UK
7 Molecular Neuromodulation, Department of Experimental Medical Science, Lund University, 22184 Lund, Sweden

Correspondence to: Tomas Björklund
Molecular Neuromodulation, Lund University, BMC, A10 22184, Lund, Sweden
E-mail: tomas.bjorklund@med.lu.se

**Keywords:** gene therapy; L-DOPA; adeno-associated viral vector; non-human primate; MPTP

**Abbreviations:** 6-OHDA = 6-hydroxydopamine; AAV = adeno-associated viral vector; LID = L-DOPA-induced dyskinesia; NHP = non-human primates; MPTP = 1-methyl-4-phenyl-1,2,3,6-tetrahydropyridine

Received February 15, 2019. Revised March 19, 2019. Accepted April 24, 2019. Advance Access publication June 26, 2019

# Introduction

Current approaches to gene therapy for patients with Parkinson's disease are based on two alternative, but potentially complementary, strategies. First, interference with the degenerative process affecting the dopamine neurons in the midbrain through the supply of neurotrophic factors, such as glial cell line-derived neurotrophic factor or neurturin, an approach previously pursued by Ceregene (Bartus *et al.*, 2015; Warren Olanow *et al.*, 2015), and now continued in an ongoing adeno-associated viral vector (AAV) glial cell line-derived neurotrophic factor trial led by investigators at the National Institute of Neurological Disorders and Stroke (NINDS) (https://clinicaltrials.gov/ct2/show/NCT01621581?term=gdnf&rank=1). Second, restoration of dopamine function in the denervated striatum can be accomplished through delivery of the three enzymes needed for the production of dopamine, i.e. tyrosine hydroxylase (TH), aromatic amino acid decarboxylase, and the cofactor-producing enzyme guanosine-5'-tri-phosphate-cyclohydrolase-1 (GCH1). This strategy, which is aimed to provide a constant supply of dopamine locally in the striatum, was initially pursued by Oxford Biomedica, and is now continued by Axovant Sciences (Palfi *et al.*, 2014, 2018). In addition, researchers at University of California San Francisco, in collaboration with Genzyme, have initiated trials using delivery of only one of the three enzymes, aromatic amino acid decarboxylase, with the goal to facilitate the conversion of orally administrated L-3,4-dihydroxyphenylalanine (L-DOPA), now continued by Voyager Therapeutics (Christine *et al.*, 2009, 2019; Mittermeyer *et al.*, 2012). Although early in development, the results obtained in these clinical phase I/II trials have been sufficiently promising to be pursued further.

The approach explored here is based on the use of an AAV vector to deliver the two L-DOPA synthesizing enzymes, TH and GCH1, aimed to provide a source of continuous L-DOPA delivery locally in the dopamine-deficient striatum. There is considerable evidence that the dyskinetic side effects of standard L-DOPA medication is caused by the excessive fluctuations in striatal dopamine caused by intermittent, pulsatile oral delivery (Olanow *et al.*, 2000, 2006). In support of this idea, it has been shown that more continuous delivery of L-DOPA, obtained by long-acting oral medication or intrajejunal infusion of L-DOPA, has proven efficient in dampening these dyskinetic side effects. As a result, new extended-release formulations and other delivery routes are now under development (for reviews see Poewe and Antonini, 2015; Timpka *et al.*, 2016).

Intrastriatal AAV-mediated enzyme delivery holds promise as a tool to provide a local source of continuous and more physiological L-DOPA delivery, thus avoiding the motor fluctuations and the dyskinetic side effects associated with standard oral L-DOPA medication. This approach is attractive also in that it delivers L-DOPA locally to the site where it is needed, i.e. in the dopamine-depleted striatum, thus avoiding the risk of off-target neuropsychiatric effects, and that it is based on a single intervention using a vector that can maintain stable expression and delivery over many years (Hadaczek *et al.*, 2010; Sehara *et al.*, 2017). An additional potential advantage is that transduction of the spiny projection neurons is likely to result in nigral L-DOPA delivery as well through the projections to the pars reticulata region, which may be functionally beneficial (Robertson, 1992).

In our previous studies we have shown that combined AAV-mediated expression of TH and GCH1 can restore dopamine production and reverse motor impairments in the 6-hydroxydopamine (6-OHDA) rat model of Parkinson's disease (Kirik *et al.*, 2002; Bjorklund *et al.*, 2009, 2010). These experiments were performed using a mixture of two AAV vectors expressing each of the two genes *TH* and *GCH1*. As a step towards clinical use, however, we developed a single vector design where both genes are co-expressed to enable efficient L-DOPA production from a single AAV vector (Cederfjall *et al.*, 2012, 2013). Based on a screening performed in both rats and non-human primates (NHP) we selected AAV5 to be the preferred serotype for gene delivery to the striatum (Dodiya *et al.*, 2010). In the experiments summarized here we explored the therapeutic efficacy of the AAV5-GCH1-TH vector in an NHP model of permanent dopaminergic depletion as seen in patients suffering from Parkinson's disease. We show that combined TH and GCH1 delivery is efficient in reversing motor impairment in 1-methyl-4-phenyl-1,2,3,6-tetrahydropyridine (MPTP)-treated rhesus macaques, and that this improvement is obtained without any adverse effect on dyskinesias induced by long-term L-DOPA treatment.

# Materials and methods

## AAV vector production

Two constructs were cloned to express human GCH1 and TH under separate promoters in a single AAV vector. The first cassette expresses GCH1 under the human synapsin 1 promoter (*SYN1*) and is terminated by the late SV40-derived polyadenylation sequence. The second expression cassette differs between the vectors. In the first vector, the *TH* gene is driven by a second *SYN1* promoter and is flanked 3′ by the Woodchuck hepatitis virus post-transcriptional regulatory element (WPRE) and terminated by a SV40-derived polyadenylation sequence. This AAV vector is named Syn1-GCH1|Syn1-TH-W. In the second vector, the *TH* gene is driven by the *CMV* promoter and is flanked 5′ by the human growth hormone intron and 3′ by the *TH* UTR and a SV40-derived polyadenylation sequence. Finally, a green fluorescent protein (GFP) control vector was generated where the *GFP* gene is driven by a *SYN1* promoter and flanked 3′ by a WPRE and polyadenylation sequence (named Syn1-GFP-W). All vectors were produced by dual-plasmid, PEI-based transient transfection of HEK-293 cells (Grimm *et al.*, 1998). Cell lysates and supernatant were then purified

using AVB Sepharose™ High Performance affinity resin. Viral titres were quantified to range between $1 \times 10^{13}$ and $1.3 \times 10^{13}$ gc/ml using quantitative (q)PCR with primers against the WPRE and *CMV* promoter, respectively.

## Animals and housing

All animal experiments were performed in accordance with the European Union directive of 22, September 2010 (2010/63/EU) on the protection of animals used for scientific purposes.

Eighteen adult, female, wild-type Sprague Dawley rats (225–250 g) were housed in standard laboratory cages with *ad libitum* access to food and water, under a 12-h day/night cycle in temperature and humidity-controlled rooms. All experimental procedures performed in this study were approved by the local ethics committee in the Malmo/Lund region 'Malmö/Lunds regionala djurförsöksetiska nämnd' in accordance with national and EU regulations.

We performed the NHP experiments in an AAALAC-accredited facility following acceptance of study design by the Institute of Lab Animal Science (Chinese Academy of Science, Beijing, China). Forty-four male rhesus macaques (*Macaca mulatta*; Xieerxin Laboratory Co. Ltd) bred in captivity were housed in an air-conditioned room under a 12-h day/night cycle. Environmental enrichment was provided in the home cages. Animals were housed in pairs to permit socialization and reduce stress. Food pellets (SAUE Ltd Old World Monkey) and drinking water were available *ad libitum* and was supplemented daily with fresh fruit and vegetables. If, at any point, an animal's condition required supplemental feeding, nutritional milk (Heinz) was given by gavage (up to three times of 100 ml per day). Animal care was supervised daily by veterinarians skilled in the healthcare and maintenance of NHPs.

## Rat surgical procedures

Rats were deeply anaesthetized using an intraperitoneal injection of fentanyl/dormitor mixture prior to all surgeries and placed in a stereotactic frame with the tooth bar individually adjusted for flat skull. Targeting coordinates for all infusions were performed in relation to the animals' bregma. The animals then received a small burr hole through the skull and were infused with solutions containing either 6-OHDA or viral vectors unilaterally into the brain using a pulled glass capillary (60–80 µm inner diameter and 120–160 µm outer diameter) attached to a 25 µl Hamilton syringe. All surgical interventions were performed on the right hemisphere of the brain and thus affect the left side of the body more severely in motor tests.

For unilateral 6-OHDA lesions of the medial forebrain bundle, 3 µl of 6-OHDA (Cl-salt, Sigma Aldrich) was diluted in 0.02% ascorbic acid and infused at a concentration of 3.5 µg/µl (free base weight) at the following coordinates: AP = −4.4; ML = −1.1; DV = −7.8 with an infusion rate of 0.3 µl/min (Ungerstedt and Arbuthnott, 1970; Carta *et al.*, 2007).

Twelve animals were selected based on significant impairment in the cylinder, stepping and corridor tests. The 12 rats were balanced into two groups based on their baseline performance in the three behaviour tests. Groups were then randomized to receive AAV5 Syn1-GCH1|Syn1-TH-W or the AAV5 Syn1-GCH1|CMV-TH vector.

AAV5 viral vectors were diluted to $1 \times 10^{12}$ gc/ml and injected into the striatum at one infusion site with two deposits at the following coordinates and volumes: AP = +0.5; ML = −3.4; DV = −5.0/−4.0 2 µl AAV total injection (1.25 µl in lower deposit and 0.75 µl upper deposit) (Cederfjall *et al.*, 2012). All viral vector solutions were injected with an infusion rate of 0.4 µl/min.

## Stepping test

We investigated the forelimb akinesia using the stepping task (Schallert *et al.*, 1979), modified to a side-stepping test by (Olsson *et al.*, 1995) at 3-weeks post 6-OHDA lesion and 8 and 12 weeks following the AAV delivery. The rats were initially trained to be held by the researcher while making adjusting forelimb steps as the animal was moved sideways across a flat surface at a constant speed for a total distance of 90 cm. The number of adjusting steps was counted by the researcher for both forehand and backhand limb steps and compared to the number of steps counted on the intact forelimb (ipsilateral to the lesion) for three consecutive trials. The researcher was blinded to both animal group and treatment.

## Cylinder test

Animals were placed in a glass cylinder (20 cm in diameter) and recorded with a digital video camera in reduced light conditions, in order to stimulate an exploratory response as described previously (Bjorklund *et al.*, 2010). Two perpendicular mirrors were placed behind the cylinder, permitting a clear recording of the animals from all angles within the cylinder. The animals were recorded for at least 30 paw touches on the walls of glass cylinder, or for a maximum of five minutes. The paw touches on the cylinder wall was then scored *post hoc* from the recordings by a blinded researcher, with the score expressed as percentage of ipsilateral (right) or contralateral (left) touches out of the number of total paw touches.

## Corridor test

The rats were placed inside a corridor (1500 × 70 × 230 mm) with 10 pairs of adjacent food bowls distributed evenly throughout the corridor with each food bowl being filled with 5–10 sugar pellets, as described previously (Dowd *et al.*, 2005). Retrievals from the food bowl were scored each time the rats poked their nose into a unique bowl. Repeated nose pokes into the same bowl without retrievals from any other bowl were not scored. The rats were tested until 20 retrievals were scored, or for a maximum of 5 min. Prior to testing the rats were trained in the corridor for several days until a stable baseline of retrievals was achieved. Before each test the rats were habituated in an empty corridor without any food bowls for 5 min. The rats were then scored by percentage ipsilateral (right) and contralateral (left) retrievals out of the total number of retrievals by a blinded researcher.

## Rat tissue preparation and immunohistochemistry

All animals were sacrificed at 12 weeks post AAV surgery by sodium pentobarbital overdose (Apoteksbolaget). The rats

were transcardially perfused with 150 ml physiological saline solution followed by 250 ml of ice cold 4% paraformaldehyde (PFA) in 0.1 M phosphate buffer (pH 7.4). The rat brains were then removed and post-fixed for 2 h before being moved to buffered sucrose (30%) for cryoprotection for at least 24 h. The brains were then frozen in dry ice and cut into coronal sections with a thickness of 35 µm using a sliding microtome (HM 450, Thermo Scientific). The brain sections were collected in eight series and stored in a 0.5 M sodium phosphate buffer, 30% glycerol and 20% ethylene glycol anti-freeze solution at −20°C.

For immunohistochemical analysis, using a standard free-floating protocol, tissue sections were washed (3 ×) with TBS (pH 7.4) and incubated for 1 h in 3% $H_2O_2$ in 0.5% Tris-buffered saline (TBS) Triton solution to quench endogenous peroxidase activity and to increase tissue permeability. Following another washing step, the sections were blocked in 5 % bovine serum and incubated for 1 h and subsequently incubated with primary monoclonal antibodies overnight.

For transgene detection, a monoclonal mouse anti-TH antibody (Millipore MAB318 at 1:1000) and a polyclonal rabbit anti-GCH1 (Abiotec 25068 at 1:500) were used as primary antibodies. Following overnight incubation, the primary antibodies were first washed off using a TBS washing step and then incubated with secondary antibodies for 2 h in TBS solution. For 3,3′-diaminobenzidine (DAB) immunohistochemistry, biotinylated anti-mouse (BA-2001, Vector Laboratories 1:250) and anti-rabbit (BA-1000, vector laboratories 1:250) secondary antibodies were used. Following incubation and another TBS wash step the brain sections were incubated with the ABC-kit (VectorLabs) to amplify the staining intensity through streptavidin-peroxidase conjugation and followed by a DAB in 0.01% $H_2O_2$ colour reaction.

## MPTP lesion

Twenty-nine macaques were injected once daily with MPTP (0.2 mg/kg, intravenous; Sigma-Aldrich) as described previously (Bezard *et al.*, 1997, 2001) while an additional four intact animals were used as controls. The progression of the syndrome (and hence the lesion) was assessed daily using a validated monkey parkinsonian rating scale (Benazzouz *et al.*, 1993; Imbert *et al.*, 2000). MPTP injections were discontinued when the animal reached a mild–moderate parkinsonism (7 points). On average, MPTP treatment duration was 25 days (range 17–47 days). Following MPTP discontinuation animals were left untreated until their parkinsonian disabilities stabilized, which was defined as a consistent Parkinson's disease score over a 2-week period. Animals that did not reach a stable parkinsonian state over the first treatment period ($n = 9$) were re-dosed according to the same regimen.

## L-DOPA-induced dyskinesia

Following stabilization of parkinsonian motor impairment, L-DOPA/benserazide, (p.o. by gavage, ratio 4:1, Madopar®, Roche) was given twice daily for 2 weeks to induce L-DOPA-induced dyskinesia (LID) as described previously (Santini *et al.*, 2010; Charron *et al.*, 2011; Porras *et al.*, 2012; Bourdenx *et al.*, 2014; Shariatgorji *et al.*, 2014; Engeln *et al.*, 2015; Napolitano *et al.*, 2017; Stanic *et al.*, 2017; Rojo-Bustamante *et al.*, 2018). The dose administered was tailored individually to a dose (mean 33.8 ± 1.7 mg/kg) that produced maximal reversal in the monkey parkinsonian rating scale, and which has been associated with the development of dyskinesia (Bezard *et al.*, 2003; Ahmed *et al.*, 2010; Fasano *et al.*, 2010; Porras *et al.*, 2012; Urs *et al.*, 2015).

## Behavioural testing

Twenty-four of 29 MPTP-treated macaques were selected for the study based on parkinsonian score, L-DOPA response and LID. Animals not showing a clear symptomatic relief from clinically relevant L-DOPA doses were excluded. Eighteen animals were selected for part 1 of the study and six animals for part 2. An additional four intact animals were used as control.

Parkinsonian disability was assessed according to the schedule outlined in Fig. 4A, by an observer blinded to treatment, from video recordings captured while animals were without L-DOPA treatment (OFF), and for 4 h following an L-DOPA treatment dose (ON) according to standard guidelines (Fox *et al.*, 2012). The parkinsonian features scored were motor (0–4), bradykinesia (0–3), posture (0–2), and tremor (0–1) as described previously (Shen *et al.*, 2015; Urs *et al.*, 2015; Ko *et al.*, 2016, 2017; Baufreton *et al.*, 2018). Dyskinesia was scored as chorea (0–4) and dystonia (0–4) (Fox *et al.*, 2012; Shen *et al.*, 2015; Urs *et al.*, 2015; Ko *et al.*, 2016, 2017; Baufreton *et al.*, 2018). The scoring was done over 10 min every 30 min, i.e. in total eight scores following a single L-DOPA administration (Fox *et al.*, 2012; Shen *et al.*, 2015; Urs *et al.*, 2015; Ko *et al.*, 2016, 2017; Baufreton *et al.*, 2018). The L-DOPA test dose used was individually tailored to the lowest dose that gives maximal recovery in motor function, defined as 100%. In addition, a higher dose (133%) was used for LID induction and a lower (67%) dose was used for L-DOPA maintenance to investigate if dyskinesia was aggravated by the AAV-TH/GCH1 treatment.

## Macaque AAV5 surgery

Stereotactic surgery for vector injection in the striatum was performed as described previously (Ahmed *et al.*, 2010; Fasano *et al.*, 2010; Porras *et al.*, 2012; Urs *et al.*, 2015). Pre- and post-surgical animal care was under supervision of a certified veterinarian. All surgeries were done under aseptic conditions with animals under general anaesthesia using ketamine (10 mg/kg, intramuscular) and isoflurane inhalation. Vital parameters were continuously monitored throughout the surgical procedure. The animal was positioned in a stereotactic surgical frame (Kopf). A burr hole was made (Dremel) into the skull without damaging the dura mater. Ventriculography was performed by injection of contrast medium (Omnipaque, Nycomed) into the anterior horn of the lateral ventricle through a ventriculographic cannula mounted on a syringe. The procedure was used to locate the borders of the third ventricle, and also the edges of the anterior and posterior commissures and the position of the anterior commissure was then combined with a stereotaxic population-based atlas (Francois *et al.*, 1996) of the basal ganglia to locate the position of the left and right putamen.

In part 1 of the study a total volume of 45 µl rAAV-TH/GCH1 or vehicle (dPBS + $MgCl_2$ and $CaCl_2$; Sigma-Aldrich) was injected into each putamen using a Hamilton syringe fitted with a 28-gauge injection needle). The volume was

injected along three tracks (two deposits/track of 7.5 µl each; AP: +1, −1 and −4 mm relative to the anterior commissura; L: ±14, 14 and 15 mm relative to midline; and DV 0 mm and +3 mm relative to the line between anterior and posterior commissura) at 2 µl/min. The total injected number of genome copies (gc) was $9 \times 10^9$ and $9 \times 10^{10}$, respectively.

In part 2 of the study the injected volume was 90 µl/putamen [12 deposits of 7.5 µl along four tracks (three, four, three, and two deposits in the anterior to posterior tracks, respectively) at the following coordinates: AP: +1, −1, −2.5 and −4 mm relative to the anterior commissura; L: ±14, 14, 14 and 15 mm relative to the midline; DV: −1, +1, +3 and +5 mm]. Each animal received a total of $9 \times 10^{11}$ gc of the AAV vector.

To look at transfection volume by intraputaminal injections, two intact animals received injections of an rAAV5-GFP vector ($1 \times 10^{11}$ gc/ml or $1 \times 10^{12}$ gc/ml; Fig. 1F′ and G) along two

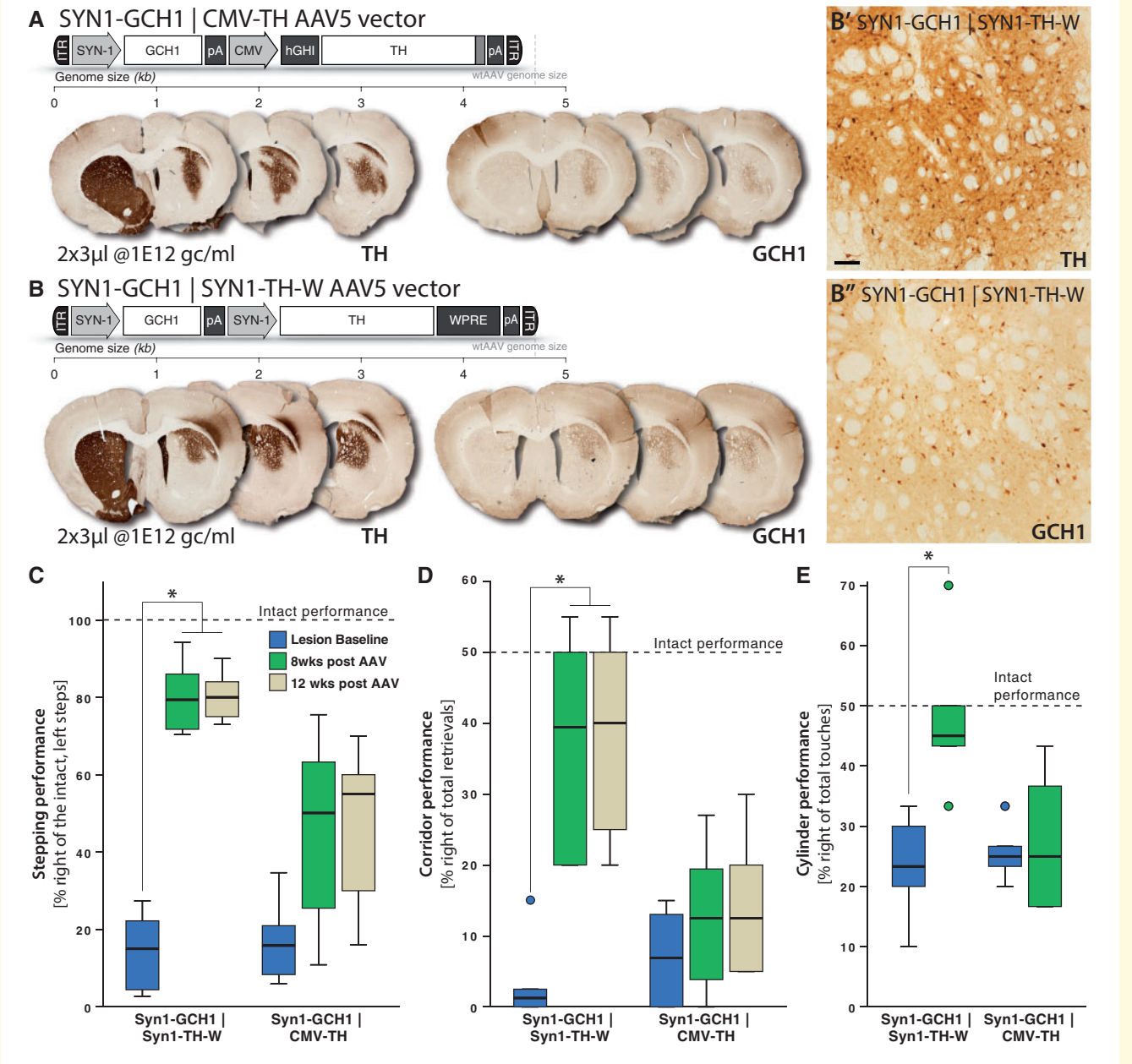


**Figure 1 Vector validation in 6-OHDA lesioned rats.** Two AAV5 vector constructs were generated which express GCH1 and TH in the same vector: Syn1-GCH1|CMV-TH (**A**) and Syn1-GCH1|Syn1-TH-W (**B**). The vectors were injected into the 6-OHDA lesioned rat striatum ($n = 6$ in each group) and the brains were processed for TH and GCH1 immunohistochemistry 12 weeks post-injection. The transduction patterns were similar for both vectors (**A** and **B**). As per the design of the vectors, TH expression (*left* in **A** and **B**) was significantly stronger than GCH1 expression (right in **A** and **B**, *top* in **B**′ and **B**″). The Syn1-GCH1|Syn1-TH-W showed superior behavioural recovery compared to the Syn1-GCH1|CMV-TH vector in all three motor tests; stepping (**C**), corridor (**D**) and cylinder test (**E**), and was thus selected for further study in the NHP experiment. In the box plots (**C**–**E**), the line represents median and the box the interquartile range (IQR). The whiskers represent the highest and lowest values which are no greater than 1.5 times the IQR. Outliers are represented as coloured circles. *Different from baseline (Tukey HSD in **C**, **D** and Student's *t*-test in **E**). Scale bar in **B**′ = 50 µm in **B**′ and **B**″.

tracks (two deposits of 7.5 µl/track; AP: ±0 and −4 mm relative to the anterior commissura; L: ±14, and 15 mm relative to midline; and DV 0 mm and +3 mm relative to the line between anterior and posterior commissure) at 2 µl/min in the rostral and caudal putamen.

To prevent infections, amoxicillin (Duphamox®, 15 mg/kg; subcutaneous) was given 1 day before surgery, and again 1 day post-surgery. Ketoprofen (Ketophen, 2 mg/kg; subcutaneous) was administered over the first 3 days post-surgery to reduce pain.

## Toxicological assessment

To assess the toxicity of this vector, we performed an acute (28 day) and a chronic (9 month) toxicology study under Good Laboratory Practice (GLP) conditions through an independent contract research organization (CRO). In these studies, the same vector batch and three vector titers ($1 \times 10^{11}$, $1 \times 10^{12}$ and $5 \times 10^{12}$ gc/ml) were assessed in two female and two male *Cynomologus* macaques. In summary, the neuropathologist's observation was that there were no changes associated with the test item in any tissue including the CNS. There were inflammatory changes associated with intrastriatal technique present in all groups and both genders. There were no lesions directly caused by the test items in the CNS. An extended summary is available upon request.

## Post-mortem tissue processing

Animals were euthanized in accordance with accepted European Veterinary Medical Association guidelines. Animals were first sedated with ketamine, (15 mg/kg, intramuscular) and then deeply anaesthetized with sodium pentobarbital (150 mg/kg, intravenous) and then perfused with saline containing heparin. The brain was rapidly removed and bisected in the midline. The left hemisphere was frozen in cold isopentane (at −50°C ± 2°C). The right hemispheres were post-fixed in 4% paraformaldehyde for a week and then transferred to sucrose solution (30%) for immunohistochemical processing.

The fixed hemispheres were sectioned coronally through the entire extent of the putamen, at a thickness of 50 µm, using a Leica cryostat, and stored in a cryopreservative solution (300 ml glycerol, 300 ml ethylene glycol, 300 ml water and 100 ml phosphate buffer 1 M) at 4°C.

## Immunohistochemistry

Free-floating sections through substantia nigra were rinsed in PBS, quenched in 0.3% $H_2O_2$ for 10 min, and incubated in PBS-BSA 1/50 (bovine serum albumin, SeraCare Life Sciences) 0.3% Triton™ X-100 buffer for 30 min to block non-specific antigen binding. Sections were then incubated overnight at room temperature in a monoclonal mouse anti-TH antibody solution (Millipore MAB318 at 1:10 000 in PBS, 1/500 BSA, 0.3% Triton™ X-100). The next morning sections were rinsed in PBS and incubated for 30 min with anti-mouse DAKO envision reagent (anti-mouse Ig peroxidase polymer detection kit, DAKO K4007). Immunological staining was then revealed with DAB (DAKO envision kit). Coronal sections were then carefully placed onto gelatine-coated glass slides and left to air dry. The dried sections were incubated overnight in a 50/50% chloroform/alcohol solution, rehydrated, counterstained with 0.1% Cresyl violet, dehydrated, and cover-slipped.

Sections through the putamen for TH and GCH1 immunohistochemistry were processed using a similar procedure, but to expose antigen epitopes, sections were incubated in citrate buffer (10 mM, pH 6) for 30 min at 80°C in a water bath following the quenching step. Sections were then incubated overnight at room temperature with a rabbit primary antibody for TH (anti-TH monoclonal C-terminus, LS-C50074) at a dilution of 1/1000, or two nights at 4°C in the same antibody buffer containing a rabbit primary antibody for GCH1 (anti-GCH1, Abiotec 25068) at a dilution of 1/500. Sections were then rinsed thoroughly in PBS and incubated for 30 min with anti-rabbit DAKO envision reagent (anti-rabbit Ig peroxidase polymer detection kit, DAKO K401111–2). Immunological staining was then revealed with DAB (DAKO envision kit). Coronal sections were then carefully placed onto gelatine-coated slides, left to air dry, dehydrated and cover-slipped.

Sections for GFP-immunohistochemistry in the two rAAV-GFP-injected animals were processed as for nigral TH immunohistochemistry above but using rabbit anti-GFP 1/1000 (Invitrogen A11122) and an Envision anti-rabbit ready to use (Dako K4002) kit.

## Stereological counting of TH-positive neurons in the substantia nigra pars compacta

Unbiased stereological analysis was used to estimate the number of TH-immunopositive neurons (Mercator, Explora Nova) as previously described (Bourdenx *et al.*, 2016). The boundaries of the SN were determined based on the Nissl staining. The volume was calculated by using the formula: $V = S\ td$; where $S$ is the sum of surface areas, $t$ is the average section thickness and $d$ is the number of slices between two consecutive sections measured. One in every 12 sections was used; optical dissectors were distributed using a systematic sampling scheme. Dissectors (100 µm length, 80 µm width) were separated from each other by 600 µm ($x$) and 400 µm ($y$). The following formula was used to estimate the number of TH-IR neurons: $n = V(SNc)\ (Q\text{-}/V(dis))$; where $n$ is the estimation of cell number, $V$ is the volume of the SNc, $Q$- is the number of cells counted in the dissectors, and $V(dis)$ is the total volume of all the dissectors. Mean estimated number of neurons and standard error of the mean (SEM) was then calculated for each group.

## Distribution volume of rAAV5 injections

After tissue processing for GFP staining, coronal sections were sampled throughout the striatum and the transduction volume was calculated with Cavalieri's principle using the Mercator image analysis system (Explora Nova), delineating the striatal boundaries on one hand and the transduced area boundaries on the other hand as described previously (Porras *et al.*, 2012; Engeln *et al.*, 2016).

## *In vitro* gene expression assay

The GCH1-TH genome was pseudotyped in an AAV2 vector (AAV5 capsid is not well suited for *in vitro* transduction), and used to transduce the neuroblastoma cell line SH-SY5Y

obtained from the American Tissue Culture Collection (ATCC). RNA extraction was performed using the RNeasy® mini Kit (Qiagen) following the manufacturer's instructions. RNA was then reverse-transcribed using the High-Capacity cDNA Reverse Transcription Kit (Applied Biosystems) following the manufacturer's instructions. 3′FAM-5′MGB-conjugated qPCR probes and qPCR primers designed to bind to *TH*, *GCH1* or *ACTB* (β-actin) genes were obtained from Thermo Fischer. Quantitative PCR was performed on cDNA using the TaqMan™ Universal PCR master mix (Life Technologies) and the custom primer-probe mix of choice; primers were used at a final concentration of 900 nM, and probes at 250 mM. Relative expression levels were determined by the ΔΔCt method.

## Statistics

Data analysis, plotting and statistics were conducted in SPSS version 23. Statistical tests included Bonferroni corrected paired Student's *t*-test when only two states or time points were compared and one-way ANOVA or two-way mixed model repeated measures ANOVA when three or more groups, states, or time points were compared. In the latter case this was followed by Levene's homogeneity test. This determined the choice of post-hoc test to either Dunnett's T3 (when Levene's fail) or Tukey's HSD. In comparisons to baseline or vehicle control group, a different from vehicle group a one-sided Dunnett *t*-test was used. Unless otherwise noted, data in figures are presented as the arithmetic mean plus and/or minus one standard error of the mean (SEM). Comparisons were considered significant when $P$-value $< 0.05$.

## Data availability

The data that support the findings of this study are available from the corresponding author, upon reasonable request.

# Results

Two AAV constructs that aimed to provide continuous L-DOPA delivery, which express GCH1 and TH from the same vector, were generated; Syn1-GCH1|Syn1-TH-W and Syn1-GCH1|CMV-TH (Syn1 = synapsin 1 promoter; W = WPRE regulatory element; CMV = cytomegalovirus promoter). The vectors show a similar transduction pattern when packaged into an AAV serotype 5 vector and injected into the striatum of rats with a complete unilateral dopamine denervation induced through a medial forebrain bundle 6-OHDA toxin injection (Fig. 1A and B). The bicistronic design of the vectors ensures that all transduced neurons contain both transgenes. This is observed as a perfect overlap in transduction pattern between TH and GCH1 immunoreactivity. While the transduction pattern is similar between the two constructs after injection of $2 \times 3$ µl AAV5 vector at $1 \times 10^{12}$ gc/ml (Fig. 1A and B), they result in significantly different motor recovery. In this lesion model of end-stage Parkinson's disease, the AAV5 Syn1-GCH1|Syn1-TH-W vector provided near complete restoration of motor function in the stepping and corridor tests (Fig. 1C and D) and complete restoration in the cylinder test (Fig. 1E). The restoration was prominent at 8 weeks and maintained at 12 weeks post AAV injection. The functional recovery for the Syn1-GCH1|CMV-TH was much less pronounced (Fig. 1C–E). Therefore, we chose to focus the further assessment of the continuous L-DOPA delivery in NHPs on the AAV5 Syn1-GCH1|Syn1-TH-W vector.

To ensure optimal delivery parameters and upscaling to the larger NHP putamen, we then performed a smaller *in vivo* assessment of AAV transduction in the intact brain using an AAV5 Syn1-GFP-W vector. This was injected at either $1 \times 10^{11}$ gc/ml or $1 \times 10^{12}$ gc/ml with an injection volume of 7.5 µl per injection site, delivered at two deposits along one needle tract (Fig. 2A and B′). Both vector doses resulted in considerable transduction in

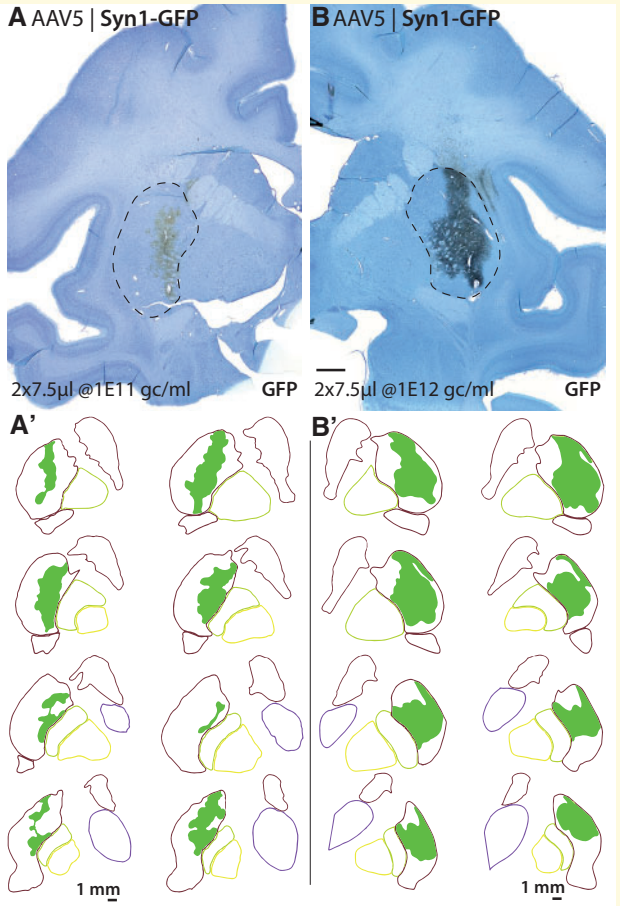


**Figure 2 Vector validation in healthy NHPs.** Serotype, target and dose validation was performed in the intact NHP putamen using the green GFP-expressing AAV5 Syn1-GFP-W vector injected at either $1 \times 10^{11}$ (A and A′) or $1 \times 10^{12}$ gc/ml (B and B′). GFP immunohistochemistry (**A** and **B**) was used to map the transduction area using camera lucida delineation (**A′** and **B′**) thereafter the transduced fraction of the total volume of the putamen was calculated (Table 1). The 10-fold increase in vector titre was reflected in an ~2-fold increase in the volume of transgene expression. Scale bar in **B** = 2 mm in **A** and **B**.

**Table 1 Vector validation in healthy NHPs**

| | Syn \| GFP at dose $1 \times 10^{11}$ gc/ml | Syn \| GFP at dose $1 \times 10^{12}$ gc/ml |
|---|---|---|
| **Normal 1** | | |
| Putamen | 447.74 ± 0.02 | 535.35 ± 0.02 |
| GFP | 59.87 ± 0.09 | 127.87 ± 0.05 |
| % volume transduced | 13.37 | 23.89 |
| **Normal 2** | | |
| Putamen | 479.64 ± 0.02 | 403.31 ± 0.02 |
| GFP | 35.20 ± 0.06 | 75.82 ± 0.06 |
| % volume transduced | 7.34 | 18.80 |

GFP immunohistochemistry (Fig. 2A and B) was used to map the transduction area using camera lucida delineation thereafter the transduced fraction of the total volume of the putamen was calculated. The 10-fold increase in vector titre was reflected in an approximately 2-fold increase in the volume of transgene expression.

a significant area of the putamen with a clear dose-related increase in both expression strength and transduction volume. A single injection tract resulted in between 7.3 and 23.9% of the putamen being transduced depending on dose and animal assessed (Table 1). For the delivery of the therapeutic vector we therefore chose to increase the needle tracts to three to four per side and deposits to two to three per needle tract depending on the target dose.

## L-DOPA responsiveness in the non-human primate MPTP lesion model

A key requirement for AAV-mediated continuous L-DOPA delivery is the availability of sufficient endogenous aromatic amino acid decarboxylase activity. Thus, the L-DOPA responsiveness of NHPs after repeated systemic MPTP administration was carefully assessed. Using the complete cohort of animals included in the study, varying doses of oral L-DOPA were assessed using both a disability rating scale and a dyskinesia rating scale. Twenty-nine were treated with systemic MPTP administration according to a strict delivery schedule to result in a moderate parkinsonian disability (24 of these were included in the vector efficacy study, as described in the 'Materials and methods' section). At 6 months after initiation of MPTP treatment, the NHPs were treated with increasing L-DOPA doses tailored to each animal. The 100% dose for each animal was individually determined to be the lowest dose needed to achieve a 75% reduction in the total disability score. After delivery of the 100% dose, the animals displayed a gradual reduction of disability until 80 min post-administration, which was maintained until 140 min post administration (Fig. 3A). Increasing the dose to 133% (the dose used to induce dyskinesia), did not result in further reduction in disability nor extended duration. Reducing the L-DOPA dose to 67% (used as a maintenance dose throughout the study) resulted in an identical peak reduction in disability at 80 min post-L-DOPA administration but the duration of the effect was substantially shorter. Plotting of the individualized doses in mg/kg L-DOPA (Fig. 3B) revealed a linear response to L-DOPA up to 30 mg/kg with an apparent ceiling effect at higher doses.

Assessment of LIDs revealed a slightly different pattern. Both magnitude of LIDs at peak therapeutic effect (50–140 min post L-DOPA) and LID duration displayed a dose-dependent increase between the 67, 100 and 133% L-DOPA treatment groups. Assessment of the area under the curve of LIDs over the entire 230 min, plotted against the individualized L-DOPA doses in milligrams per kilogram, shows however a similar linear relationship to L-DOPA dose to that of the disability scores (Fig. 3D) with a ceiling effect observed above 35 mg/kg.

## Assessment of AAV-mediated continuous L-DOPA delivery in the non-human primate MPTP model

Twenty-four male rhesus macaques, rendered parkinsonian by daily systemic MPTP treatment (Bezard *et al.*, 1997, 2001), were included in the study. We used a mixed experimental design including three active treatment groups ($n = 6$ each), a vehicle treated lesion control group ($n = 6$), and a smaller group of intact controls ($n = 4$), as shown in Fig. 4A. One AAV treatment group ($n = 6$) was used to explore a re-dosing paradigm, increasing the dose 100-fold, from $9 \times 10^9$ gc/ml to $9 \times 10^{11}$ gc/ml, simulating a clinical scenario where patients entering early in the safety trial could be offered a therapeutic dose at the end of the trial. For the second dose, this group received a slightly modified vector where the N-terminal regulatory domain of TH was removed (tTH). This truncated *TH* gene has been evaluated in clinic trials performed by Oxford Biomedica (Palfi *et al.*, 2014). The rationale for using this variant is to avert feedback inhibition of TH via its N-terminal regulatory domain by the newly synthesized dopamine accumulating in the cytosol. However, L-DOPA is known to be a much weaker inhibitor of TH, which explains why we have not seen any indication of inhibition *in vitro* or in the rodent brain. Regardless, it was important to confirm this in a clinically relevant model; a truncated TH vector was therefore included as a separate treatment group. We did not see any differences in behavioural improvement or TH immunostaining using this vector compared to the full-length variant. The third treatment group ($n = 6$) acted as a delayed start group, receiving the therapy one year after the MPTP treatment.

To assess the therapeutic potential of AAV-mediated continuous L-DOPA delivery, we focused the behavioural analysis on the assessment of global motor function, summarized in a motor score, using a scale from 0 to 4, where 4 represents normal motor behaviour. At MPTP baseline, the lesioned animals averaged 2.8 on this scale and oral L-DOPA medication induced a recovery to 3.7 at 80 min post-medication. Interestingly, all treatment

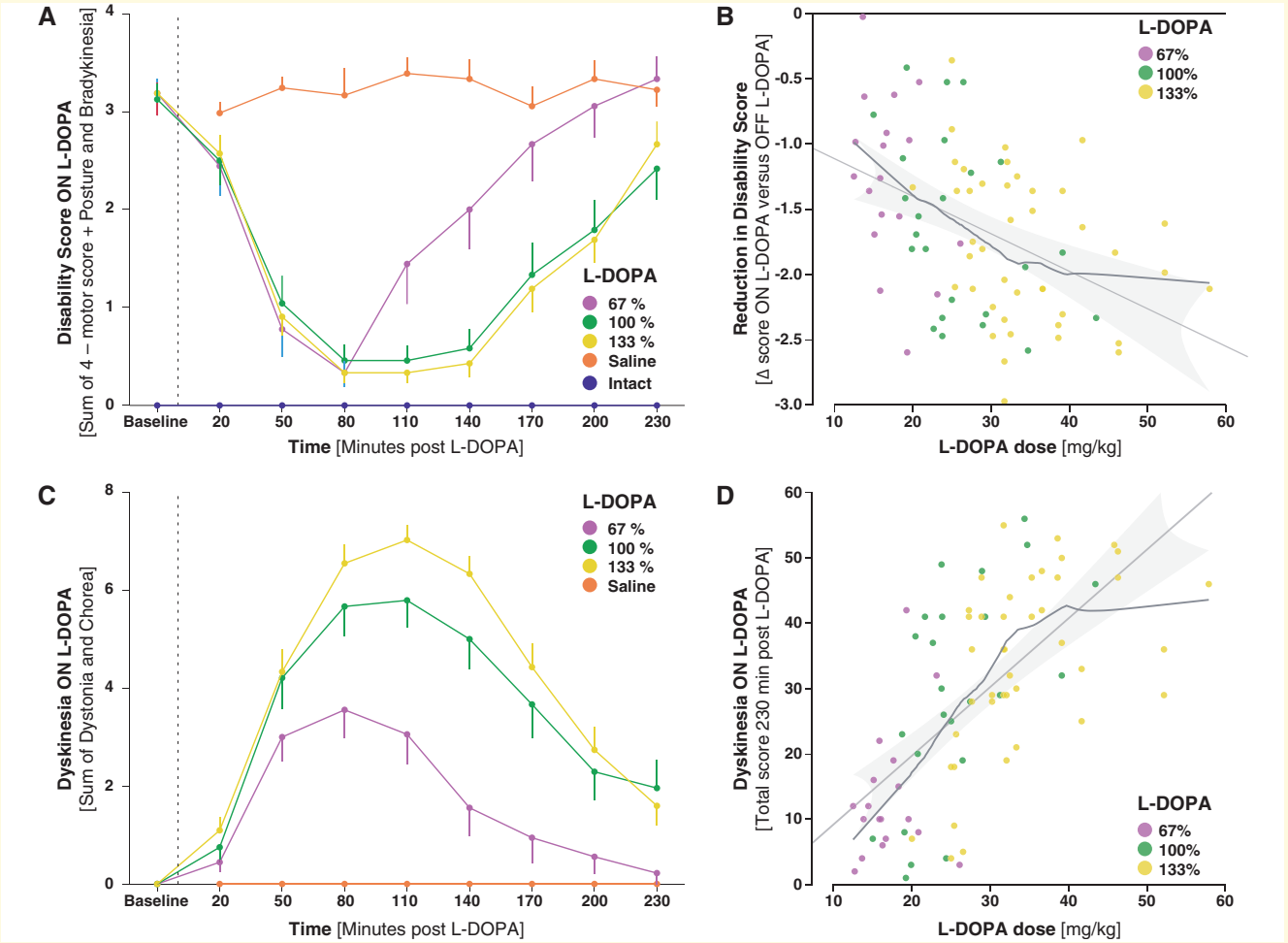


**Figure 3 Assessment of motor impairments and L-DOPA responsiveness in the MPTP-treated NHPs.** At 5 months post MPTP induction of parkinsonism, the animals were assessed for reversal of motor disability (**A** and **B**) and L-DOPA induced dyskinesias (**C** and **D**) using three different doses of the drug (67%, 100% and 133%), where 100% was defined individually for each animal as the lowest dose inducing maximal recovery in motor function. Peak reduction in disability did not significantly differ between the three L-DOPA doses, while the duration of the response was notably shorter at the lowest dose (**A**). As evident from the scatter plot in **B**, the effect reached a plateau at a dose of ~30 mg/kg (**B**). The response to L-DOPA in the form of dyskinesias was clearly dose-dependent, showing an increase in both peak and duration with increasing doses of L-DOPA (**C**). Also, in this case, the scatter plot in **D** suggests that the dyskinetic response reaches a plateau at doses above 35 mg/kg.

doses, 67%, 100% and 133% induced the same peak recovery while the 100% and 133% L-DOPA doses displayed a longer duration of improved motor function (Fig. 4B). This suggests a ceiling effect for the effect of peripheral L-DOPA on the reversal of motor deficits.

Motor score was assessed monthly pre- and post-AAV injection both OFF and ON oral L-DOPA (the 67% maintenance dose). OFF L-DOPA, the lesioned vehicle-treated monkeys displayed a spontaneous recovery up to an average motor score of 3.0. The $9 \times 10^9$ gc AAV treatment group displayed an identical recovery trajectory over the 5 months assessed (Fig. 4C). The animals in the higher dose treatment group ($9 \times 10^{10}$ gc) showed a strikingly increased rate of recovery which plateaued at an average of 3.7 in the motor score OFF L-DOPA at 3 months post-AAV injection (blue curve in Fig. 4C and D). Of note is that this level of recovery is identical to that observed in the dose escalation of peripheral L-DOPA as shown in Fig. 4B.

To assess if the recovery in motor function could be further increased, we used a 10-fold higher treatment dose ($9 \times 10^{11}$ gc). This was used both to re-dose the animals in the original low-dose group ($9 \times 10^9$ gc) and to treat a third group of six MPTP lesioned monkeys. Both treatment groups showed significant recovery over the first 2 months, reaching the same plateau as the $9 \times 10^{10}$ gc treatment group (green and black curves in Fig. 4C and E).

A major safety concern for any therapy involving long-term delivery of dopaminergic treatment is the induction or aggravation of LIDs. Therefore, the animals where primed with a daily high dose L-DOPA treatment (133%) for 1 month prior to the AAV delivery. This resulted in a dose-related increase in peak dose LIDs, ranging from around

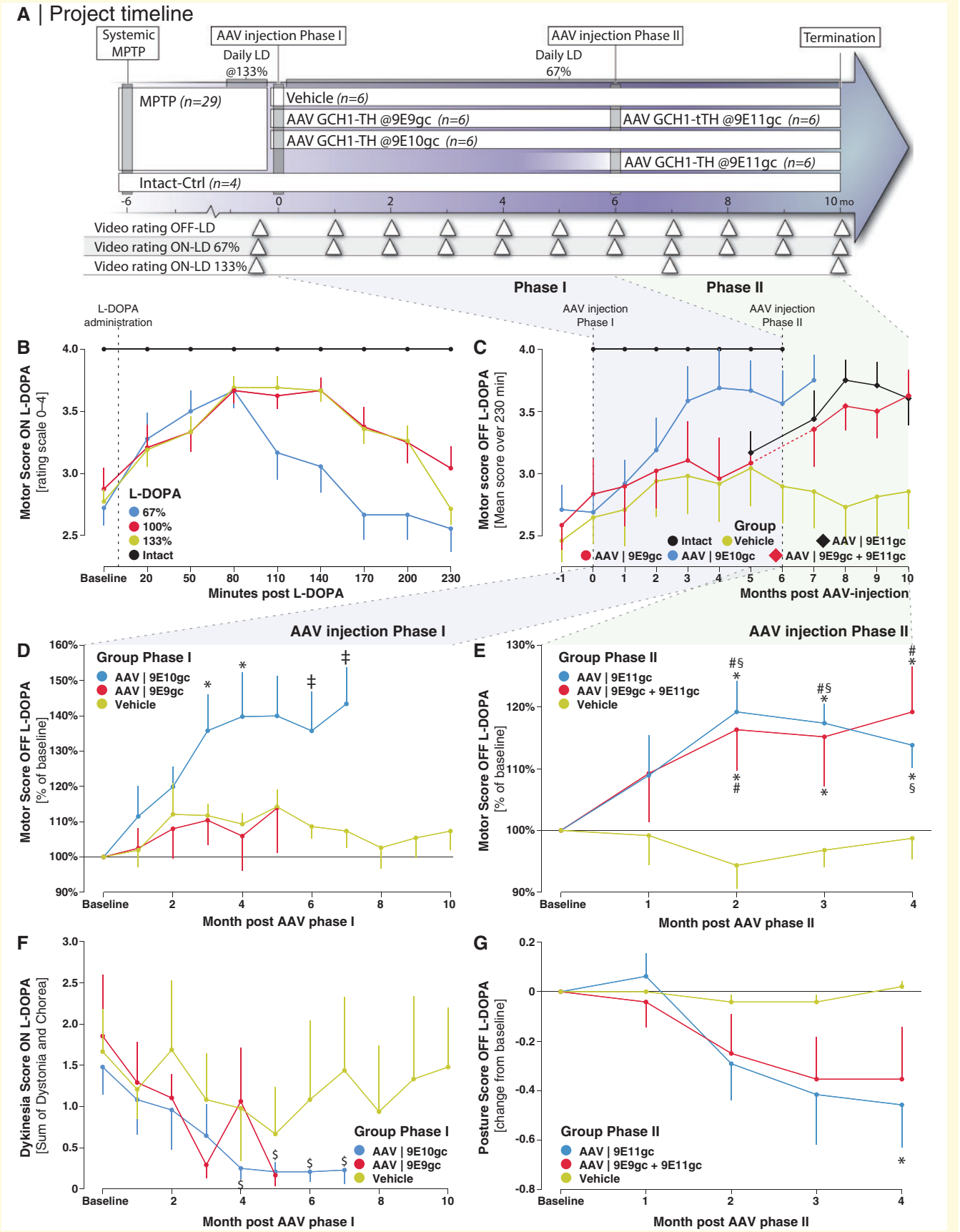


**Figure 4 Project timeline and behavioural recovery after AAV-mediated continuous L-DOPA delivery in MPTP-treated NHPs.** (**A**) Project timeline, showing the design of the two experimental phases (Phase I and II) and the allocation of the MPTP treated NHPs to the four

(continued)

3.5 for the 67% L-DOPA dose, to around 7 for the 133% dose. The LIDs were maintained throughout the study using a daily 67% L-DOPA maintenance dose. While all animals showed a variable LID score post-AAV injection, the vehicle group stayed dyskinetic throughout the 10 months of study (Fig. 4F). In contrast, the animals in the $9 \times 10^{10}$ gc group showed a significant decrease in LIDs compared to baseline, indicating that the vector-mediated DOPA delivery does not aggravate pre-existing LIDs and may in fact have the capacity of LID reversal.

An additional feature of the MPTP lesion NHP model is the induction of postural instability, which was assessed here by a posture score. At baseline, post MPTP, the animals averaged a score of 1 in this rating scale. While the animals receiving the two lower doses, $9 \times 10^{9}$ gc and $9 \times 10^{10}$ gc, showed no tendency to improvement in posture, the animals receiving the highest AAV dose ($9 \times 10^{11}$ gc) showed a gradual improvement, reaching significance at 4 months post AAV delivery (Fig. 4G).

## Post-mortem histological assessment of transgene expression and lesion severity

After the last behaviour assessment, the animals were euthanized, and the brain tissue was formalin-fixed for immunohistochemical assessment of transgene expression and lesion severity. Coronal sections from an intact forebrain stained for TH (Fig. 5A) and GCH1 (Fig. 5C) were used for comparison. As the GCH1 antibody used here does not react with endogenous GCH1, we could use immunostaining of this protein to unambiguously assess transgene expression from the vector. As the animals receiving the lowest dose ($9 \times 10^{9}$ gc) were re-dosed, only the mid- (Fig. 5D) and high-dose (Fig. 5E) specimens were available for immunostaining. In both cases the transduction was clearly visible, showing a dose-dependent increase in both intensity and transduced volume of the putamen that was very similar to the transduction pattern seen in the animals receiving the GFP-expressing test vector, shown in Fig. 2 and Table 1. Based on the rodent data, we expected a significantly stronger immunoreactivity towards the TH antigen compared to that of GCH1. However, this was not the case in the NHP putamen. While the area of the putamen displaying TH+ neurons around the injection tract closely matched the area covered by GCH1+ neurons in the adjacent section (Fig. 5G and H) the number of neurons and overall expression level was much lower in the TH staining compared to the GCH1 staining (Fig. 5G′ and H′). Of note, while the TH+ neurons express the transgene at a reasonably high level, they only represent a subset of the GCH1+ neurons (Fig. 5K–R). Moreover, they were evenly distributed throughout the transduction volume and did not follow the expected transduction gradient away from the injection tract. These TH+ neurons were not detected in the lesion control animals (Fig. 5I) or in intact putamen (Fig. 5J). Judged by their morphology (e.g. top neurons in Fig. 5G′) and abundance (observed in GCH1 staining), the majority of transduced cells were identified as medium spiny projection neurons.

To assess if this marked difference in protein expression could be due to a deficient mRNA expression of the *TH* transgene, we assessed the expression from our two gene vector using reverse transcriptase-qPCR (RT-qPCR) in a human neuroblast cell line (SH-SY5Y) transduced with the therapeutic vector. At least in this model, *TH* mRNA levels were much higher than GCH1 levels. Fold increase of expression compared to control cells was 760- to 5600-fold for *TH* and 1.2- to 1.5-fold for *GCH1*. By design, *TH* mRNA levels are expected to be much higher than *GCH1* mRNA levels due to the gene order and WPRE sequence on the *TH* transcript (Cederfjall *et al.*, 2012). Thus, our data indicate that post-transcriptional events are limiting TH protein detection. However, further investigations are warranted to determine the exact mechanism.

Lastly, we assessed the magnitude of dopamine denervation in the MPTP treated animals through stereological cell counts of the substantia nigra. Systemic MPTP treatment resulted in a loss of TH+ neurons in the substantia nigra ranging from 56 to 91% with an overall average of 78% (Fig. 5F). All lesioned groups differed significantly from the intact animals, while the MPTP treatment groups did not differ from each other.

**Figure 4** Continued

experimental groups. (**B** and **C**) Side-by-side comparison between behavioural recovery (assessed by motor score component of the disability rating scale) seen after increasing doses of peripheral L-DOPA at baseline (post MPTP, pre-AAV) (**B**), and the recovery observed after AAV-mediated continuous L-DOPA delivery (**C**). The magnitude of recovery seen with the $9 \times 10^{10}$ gc vector dose (blue curve in **C**) was closely similar to that obtained with the optimal L-DOPA dose (red and green curves in **B**). A 10-fold higher dose of the vector ($9 \times 10^{11}$ gc) provided similar magnitude of therapeutic effect (black curve in **C** and blue curve in **E**), and readministration of the AAV vector did not diminish this therapeutic potential (green curve in **C** and red curve in **E**). (**F**) Assessment of L-DOPA induced dyskinesias (LIDs) pre- and post-AAV in Phase I. Dyskinesias were significantly reduced compared to baseline in the $9 \times 10^{10}$ gc active treatment group, while they were not significantly changed in the control group. (**G**) Assessment of postural disability performed in Phase II showed gradual improvement in posture for the $9 \times 10^{11}$ gc treatment groups. This effect reached significance at 4 months post AAV injection. #Different from vehicle group (Tukey HSD). §Different from vehicle group (Dunnett T3). *Different from vehicle group (one sided Dunnett T). ‡Different from vehicle group (Students *t*-test). $Different from baseline (one sided Dunnett T).

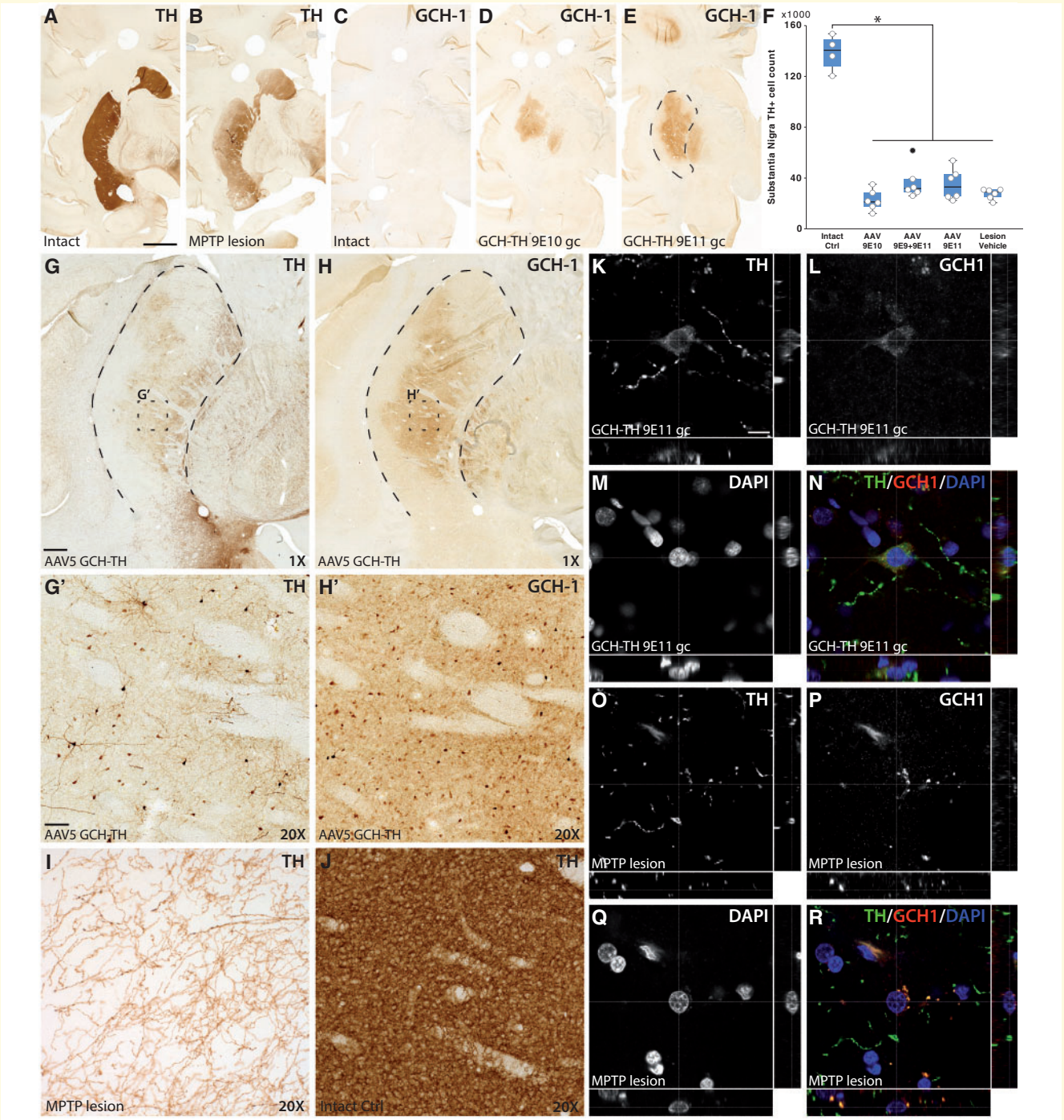


**Figure 5 Post-mortem analysis of transgene expression and lesion severity.** (**A** and **B**) NHP endogenous dopaminergic innervation of the putamen displayed strong immunoreactivity for TH, which is significantly reduced by the MPTP toxin. (**C**) The endogenous GCH1 is not recognized by the antibody raised against the human protein. (**D** and **E**) Increasing doses of the AAV5 Syn1-GCH1|Syn1-TH-W vector ($9 \times 10^{10}$ and $9 \times 10^{11}$ gc respectively) resulted in strong immunohistochemistry reactivity for GCH1 with a dose-dependent intensity and coverage. (**F**) The MPTP lesion resulted in a substantial loss of TH + neurons in the substantia nigra, ranging from 56 to 91% in the individual animals, as assessed by stereological cell counting. (**G** and **H**) Expression of TH was notably much weaker than that of GCH1, which is in contrast to the transduction pattern obtained in the rat striatum where TH was more highly expressed (see Fig. 1A and B). Although the transduced area was similar for the two proteins, as shown in **G** and **H**, the number of transduced cells with high TH expression (**G′**) was significantly lower than those expressing GCH1 (**H′**). The images shown in **G**–**H′** are from a representative animal from the highest vector dose group ($9 \times 10^{11}$ gc). (**I**) In the MPTP lesioned putamen the TH + innervation was partially spared compared to intact control (**J**), but we did not observe any TH-immunoreactive neuronal profiles similar to those seen in the AAV-injected animals. (**K**–**R**) orthogonal projection of confocal imaging stacks showing TH and human GCH1 expression in the transduced putamen (**K**–**N**) which is absent in the MPTP lesion Ctrl (**O**–**R**). In the box plots, the line represents median and the box the IQR. The whiskers represent the highest and lowest values that are no greater than 1.5 times the IQR. Outliers are represented as coloured circles. *Different from the intact group (Tukey HSD). Scale bar in **A** represents 5 mm in **A**–**E**; **G** = 1 mm in **G**–**H**; **G′** = 100 μm in **G′**, **H′**, **I** and **J**; and **K** = 10 μm in **K**–**R**.

# Discussion

The results show that the AAV-GCH1-TH vector, injected bilaterally into the putamen, induced a significant improvement of motor behaviour in the MPTP treated macaques. The effect was dose-dependent, developed gradually over 3–4 months, and remained stable thereafter. The level of improvement seen at the highest treatment dose was identical to that obtained with the optimal dose of peripheral L-DOPA.

Importantly, the improvement in motor function was obtained without any adverse dyskinetic effects, either ON or OFF oral L-DOPA. In this experiment, animals where primed with a daily high dose of L-DOPA (33% above the standard, functional dose) for 1 month prior to AAV delivery. While the control (vehicle) group remained dyskinetic throughout the 10 months of study, the AAV-treated animals in the highest dose group showed a significant decrease in LIDs compared to pre-treatment baseline, indicating that the continuous AAV-mediated L-DOPA delivery did not aggravate pre-existing LIDs. Indeed, the trend seen in this experiment suggests that the treatment may have the capacity to reduce already established dyskinesia.

We included one treatment group where we assessed a re-dosing paradigm, (increasing the dose 100-fold), as to simulate a clinical scenario where patients entering early in the safety trial could, at a later stage be offered a second therapeutic dose. These monkeys received initially the lowest (non-effective) dose, followed 6 months later by a 100-fold larger dose. The re-dosed animals showed a significant recovery over the following 2 months, reaching the same level of recovery as the initial high-dose treatment group.

The efficacy of our L-DOPA-producing vector will be limited by the access to endogenous AADC in the host brain. This is advantageous in that L-DOPA produced by our treatment vector will be converted to dopamine at the site where it is needed, and released in an efficient and physiological manner, not only from spared dopaminergic terminals but also as a 'false' transmitter from the serotonergic neurons (Tanaka *et al.*, 1999; Carta *et al.*, 2007; Navailles *et al.*, 2010). In addition, this affords a degree of safety since the level of dopamine production will be limited by the availability of AADC regardless of the rate of vector-derived L-DOPA production. It is likely, therefore, that the therapeutic effect of the AAV-GCH1-TH vector will be at the same level as the optimal response to oral L-DOPA seen in each individual. This was indeed the case here: the motor improvement seen at the highest vector dose matched well the optimal effect seen in response to increasing doses of oral L-DOPA.

It is interesting to compare the therapeutic efficacy of our AAV-GCH1-TH vector with the results reported in the study by Jarraya *et al.* (2009), which was performed in a NHP MPTP model similar to the one used here using a lentiviral vector (ProSavin) expressing all three enzymes, TH, AADC and GCH1. The ability of this vector to produce dopamine independent of the decarboxylating capacity of the host striatum could, in principle, make the ProSavin approach more efficient and scalable than the one using an L-DOPA producing construct. Nevertheless, the outcome is rather similar. In the study by Jarraya *et al.* the effect was observed sooner, developing over the first 6 weeks, but the magnitude of improvement relative to the optimal L-DOPA response was at the same level as seen here. Differences in kinetics are, however, to be expected between lentiviral and AAV vectors as the former result in transgene expression at a much faster rate both *in vitro* and *in vivo*.

The prominent effect on the MPTP-induced motor impairment is consistent with a therapeutic level of L-DOPA production. Based on the rodent data we expected that the immunoreactivity towards the TH antigen would be stronger than that of GCH1. However, this was not the case in the NHP putamen. Although the area covered by the TH- and GCH1-immunopositive neurons were closely similar, clear TH+ immunostaining was observed only in a subset of the GCH1-positive neurons, and the overall staining level was much lower. This is a concern, and we do not know how to explain this species difference in expression of the TH protein, as apparent in the immunostained sections. As endogenous TH was well-stained in the host dopamine neurons and terminals it does not seem to be a simple technical issue. Rather, it seems more likely that it could be caused by some property or regulatory feature intrinsic to the putaminal neurons of the macaque, not present in the rodent striatum. It is notable that the TH immunostaining pattern we see here in the transduced putamen (see Fig. 5G and H′) is rather similar to the TH staining pattern obtained by Jarraya *et al.* using their tricistronic lentiviral vector (see Figure 2C and D in Jarraya *et al.*, 2009). Nevertheless, we cannot exclude that this property of our vector is due to some feature of its design. If so, there may be room for further optimization of the vector construct to improve its performance in the primate striatum.

In summary, the results obtained in this study provide proof-of-principle for AAV-mediated L-DOPA delivery as a therapeutic strategy for Parkinson's disease. This refined version of classic L-DOPA treatment is attractive in that it is based on a single intervention and targeted to the site in the brain where dopamine is most needed, i.e. the striatum. The constant local supply of L-DOPA obtained with this approach holds promise as a therapeutic intervention that can provide long-lasting clinical improvement and, in the best cases, also avoid the appearance of motor fluctuations and dyskinetic side effects associated with standard oral dopaminergic medication. This gene therapy approach may thus offer the possibility to prolong and sustain the 'good years' many patients with Parkinson's disease experience during the initial stages of L-DOPA therapy.

# Acknowledgements

We acknowledge the expert experimental support of B. Mattsson, H. Li, Y. Cheng, Y. Zhang and R. Xing.

# Funding

This work was funded by Genepod Therapeutics AB where C.R., A.B. and T.B. are founders. The company retains no intellectual property or financial interest related to this gene therapy approach.


# Competing interests

The authors declare that they have no competing financial interests.

# References


Ahmed MR, Berthet A, Bychkov E, Porras G, Li Q, Bioulac BH, et al. Lentiviral overexpression of GRK6 alleviates L-dopa-induced dyskinesia in experimental Parkinson's disease. Sci Transl Med 2010; 2: 28ra.

Bartus RT, Kordower JH, Johnson EM Jr, Brown L, Kruegel BR, Chu Y, et al. Post-mortem assessment of the short and long-term effects of the trophic factor neurturin in patients with alpha-synucleinopathies. Neurobiol Dis 2015; 78: 162–71

Baufreton J, Milekovic T, Li Q, McGuire S, Moraud EM, Porras G, et al. Inhaling xenon ameliorates l-dopa-induced dyskinesia in experimental Parkinsonism. Mov Disord 2018; 33: 1632–42.

Benazzouz A, Gross C, Feger J, Boraud T, Bioulac B. Reversal of rigidity and improvement in motor performance by subthalamic high-frequency stimulation in MPTP-treated monkeys. Eur J Neurosci 1993; 5: 382–9.

Bezard E, Dovero S, Prunier C, Ravenscroft P, Chalon S, Guilloteau D, et al. Relationship between the appearance of symptoms and the level of nigrostriatal degeneration in a progressive 1-methyl-4-phenyl-1,2,3,6-tetrahydropyridine-lesioned macaque model of Parkinson's disease. J Neurosci 2001; 21: 6853–61.

Bezard E, Ferry S, Mach U, Stark H, Leriche L, Boraud T, et al. Attenuation of levodopa-induced dyskinesia by normalizing dopamine D3 receptor function. Nat Med 2003; 9: 762–7.

Bezard E, Imbert C, Deloire X, Bioulac B, Gross CE. A chronic MPTP model reproducing the slow evolution of Parkinson's disease: evolution of motor symptoms in the monkey. Brain Res 1997; 766: 107–12.

Bjorklund T, Carlsson T, Cederfjall EA, Carta M, Kirik D. Optimized adeno-associated viral vector-mediated striatal DOPA delivery restores sensorimotor function and prevents dyskinesias in a model of advanced Parkinson's disease. Brain 2010; 133: 496–511.

Bjorklund T, Hall H, Breysse N, Soneson C, Carlsson T, Mandel RJ, et al. Optimization of continuous in vivo DOPA production and studies on ectopic DA synthesis using rAAV5 vectors in Parkinsonian rats. J Neurochem 2009; 111: 355–67.

Bourdenx M, Dovero S, De Deurwaerdere P, Li Q, Bezard E. Early prenatal exposure to MPTP does not affect nigrostrial neurons in macaque monkey. Synapse 2016; 70: 52–6.

Bourdenx M, Nilsson A, Wadensten H, Falth M, Li Q, Crossman AR, et al. Abnormal structure-specific peptide transmission and processing in a primate model of Parkinson's disease and l-DOPA-induced dyskinesia. Neurobiol Dis 2014; 62: 307–12.

Carta M, Carlsson T, Kirik D, Bjorklund A. Dopamine released from 5-HT terminals is the cause of L-DOPA-induced dyskinesia in Parkinsonian rats. Brain 2007; 130: 1819–33.

Cederfjall E, Nilsson N, Sahin G, Chu Y, Nikitidou E, Bjorklund T, et al. Continuous DOPA synthesis from a single AAV: dosing and efficacy in models of Parkinson's disease. Sci Rep 2013; 3: 2157.

Cederfjall E, Sahin G, Kirik D, Bjorklund T. Design of a single AAV vector for coexpression of TH and GCH1 to establish continuous DOPA synthesis in a rat model of Parkinson's disease. Mol Ther 2012; 20: 1315–26.

Charron G, Doudnikoff E, Laux A, Berthet A, Porras G, Canron MH, et al. Endogenous morphine-like compound immunoreactivity increases in parkinsonism. Brain 2011; 134: 2321–38.

Christine CW, Bankiewicz KS, Van Laar AD, Richardson RM, Ravina B, Kells AP, et al. MRI-guided phase 1 trial of putaminal AADC gene therapy for Parkinson's disease. Ann Neurol 2019; 85: 704–14.

Christine CW, Starr PA, Larson PS, Eberling JL, Jagust WJ, Hawkins RA, et al. Safety and tolerability of putaminal AADC gene therapy for Parkinson disease. Neurology 2009; 73: 1662–9.

Dodiya HB, Bjorklund T, Stansell J III, Mandel RJ, Kirik D, Kordower JH. Differential transduction following basal ganglia administration of distinct pseudotyped AAV capsid serotypes in nonhuman primates. Mol Ther 2010; 18: 579–87.

Dowd E, Monville C, Torres EM, Dunnett SB. The Corridor Task: a simple test of lateralised response selection sensitive to unilateral dopamine deafferentation and graft-derived dopamine replacement in the striatum. Brain Res Bull 2005; 68: 24–30.

Engeln M, Bastide MF, Toulme E, Dehay B, Bourdenx M, Doudnikoff E, et al. Selective inactivation of striatal FosB/DeltaFosB-expressing neurons alleviates L-DOPA-induced dyskinesia. Biol Psychiatry 2016; 79: 354–61.

Engeln M, De Deurwaerdere P, Li Q, Bezard E, Fernagut PO. Widespread monoaminergic dysregulation of both motor and non-motor circuits in Parkinsonism and dyskinesia. Cereb Cortex 2015; 25: 2783–92.

Fasano S, Bezard E, D'Antoni A, Francardo V, Indrigo M, Qin L, et al. Inhibition of Ras-guanine nucleotide-releasing factor 1 (Ras-GRF1) signaling in the striatum reverts motor symptoms associated with L-dopa-induced dyskinesia. Proc Natl Acad Sci U S A 2010; 107: 21824–9.

Fox SH, Johnston TH, Li Q, Brotchie J, Bezard E. A critique of available scales and presentation of the non-human primate dyskinesia rating scale. Mov Disord 2012; 27: 1373–8.

Francois C, Yelnik J, Percheron G. A stereotaxic atlas of the basal ganglia in macaques. Brain Res Bull 1996; 41: 151–8.

Grimm D, Kern A, Rittner K, Kleinschmidt JA. Novel tools for production and purification of recombinant adenoassociated virus vectors. Hum Gene Ther 1998; 9: 2745–60.

Hadaczek P, Eberling JL, Pivirotto P, Bringas J, Forsayeth J, Bankiewicz KS. Eight years of clinical improvement in MPTP-lesioned primates after gene therapy with AAV2-hAADC. Mol Ther 2010; 18: 1458–61.

Imbert C, Bezard E, Guitraud S, Boraud T, Gross CE. Comparison of eight clinical rating scales used for the assessment of MPTP-induced Parkinsonism in the Macaque monkey. J Neurosci Methods 2000; 96: 71–6.

Jarraya B, Boulet S, Ralph GS, Jan C, Bonvento G, Azzouz M, et al. Dopamine gene therapy for Parkinson's disease in a nonhuman primate without associated dyskinesia. Sci Transl Med 2009; 1: 2ra4.

Kirik D, Georgievska B, Burger C, Winkler C, Muzyczka N, Mandel RJ, et al. Reversal of motor impairments in Parkinsonian rats by continuous intrastriatal delivery of L-dopa using rAAV-mediated gene transfer. Proc Natl Acad Sci U S A 2002; 99: 4708–13.

Ko WKD, Camus SM, Li Q, Yang J, McGuire S, Pioli EY, et al. An evaluation of istradefylline treatment on Parkinsonian motor and cognitive deficits in 1-methyl-4-phenyl-1,2,3,6-tetrahydropyridine (MPTP)-treated macaque models. Neuropharmacology 2016; 110: 48–58.

Ko WKD, Li Q, Cheng LY, Morelli M, Carta M, Bezard E. A preclinical study on the combined effects of repeated eltoprazine and preladenant treatment for alleviating L-DOPA-induced dyskinesia in Parkinson's disease. Eur J Pharmacol 2017; 813: 10–6.

Mittermeyer G, Christine CW, Rosenbluth KH, Baker SL, Starr P, Larson P, et al. Long-term evaluation of a phase 1 study of

AADC gene therapy for Parkinson's disease. Hum Gene Ther 2012; 23: 377–81.

Napolitano F, Booth Warren E, Migliarini S, Punzo D, Errico F, Li Q, et al. Decreased Rhes mRNA levels in the brain of patients with Parkinson's disease and MPTP-treated macaques. PLoS One 2017; 12: e0181677.

Navailles S, Bioulac B, Gross C, De Deurwaerdere P. Serotonergic neurons mediate ectopic release of dopamine induced by L-DOPA in a rat model of Parkinson's disease. Neurobiol Dis 2010; 38: 136–43.

Olanow CW, Obeso JA, Stocchi F. Continuous dopamine-receptor treatment of Parkinson's disease: scientific rationale and clinical implications. Lancet Neurol 2006; 5: 677–87.

Olanow W, Schapira AH, Rascol O. Continuous dopamine-receptor stimulation in early Parkinson's disease. Trends Neurosci 2000; 23: S117–26.

Olsson M, Nikkhah G, Bentlage C, Bjorklund A. Forelimb akinesia in the rat Parkinson model: differential effects of dopamine agonists and nigral transplants as assessed by a new stepping test. J Neurosci 1995; 15: 3863–75.

Palfi S, Gurruchaga JM, Ralph GS, Lepetit H, Lavisse S, Buttery PC, et al. Long-term safety and tolerability of ProSavin, a lentiviral vector-based gene therapy for Parkinson's disease: a dose escalation, open-label, phase 1/2 trial. Lancet 2014; 383: 1138–46.

Palfi S, Gurruchaga JM, Lepetit H, Howard K, Ralph GS, Mason S, et al. Long-term follow-up of a phase I/II study of prosavin, a lentiviral vector gene therapy for Parkinson's disease. Hum Gene Ther Clin Dev 2018; 29: 148–55.

Poewe W, Antonini A. Novel formulations and modes of delivery of levodopa. Mov Disord 2015; 30: 114–20.

Porras G, Berthet A, Dehay B, Li Q, Ladepeche L, Normand E, et al. PSD-95 expression controls L-DOPA dyskinesia through dopamine D1 receptor trafficking. J Clin Invest 2012; 122: 3977–89.

Robertson HA. Dopamine receptor interactions: some implications for the treatment of Parkinson's disease. Trends Neurosci 1992; 15: 201–6.

Rojo-Bustamante E, Abellanas MA, Clavero P, Thiolat ML, Li Q, Luquin MR, et al. The expression of cannabinoid type 1 receptor and 2-arachidonoyl glycerol synthesizing/degrading enzymes is altered in basal ganglia during the active phase of levodopa-induced dyskinesia. Neurobiol Dis 2018; 118: 64–75.

Santini E, Sgambato-Faure V, Li Q, Savasta M, Dovero S, Fisone G, et al. Distinct changes in cAMP and extracellular signal-regulated protein kinase signalling in L-DOPA-induced dyskinesia. PLoS One 2010; 5: e12322.

Schallert T, De Ryck M, Whishaw IQ, Ramirez VD, Teitelbaum P. Excessive bracing reactions and their control by atropine and L-DOPA in an animal analog of Parkinsonism. Exp Neurol 1979; 64: 33–43.

Sehara Y, Fujimoto KI, Ikeguchi K, Katakai Y, Ono F, Takino N, et al. Persistent expression of dopamine-synthesizing enzymes 15 years after gene transfer in a primate model of Parkinson's disease. Hum Gene Ther Clin Dev 2017; 28: 74–9.

Shariatgorji M, Nilsson A, Goodwin RJ, Kallback P, Schintu N, Zhang X, et al. Direct targeted quantitative molecular imaging of neurotransmitters in brain tissue sections. Neuron 2014; 84: 697–707.

Shen W, Plotkin JL, Francardo V, Ko WK, Xie Z, Li Q, et al. M4 muscarinic receptor signaling ameliorates striatal plasticity deficits in models of L-DOPA-induced dyskinesia. Neuron 2015; 88: 762–73.

Stanic J, Mellone M, Napolitano F, Racca C, Zianni E, Minocci D, et al. Rabphilin 3A: A novel target for the treatment of levodopa-induced dyskinesias. Neurobiol Dis 2017; 108: 54–64.

Tanaka H, Kannari K, Maeda T, Tomiyama M, Suda T, Matsunaga M. Role of serotonergic neurons in L-DOPA-derived extracellular dopamine in the striatum of 6-OHDA-lesioned rats. Neuroreport 1999; 10: 631–4.

Timpka J, Mundt-Petersen U, Odin P. Continuous dopaminergic stimulation therapy for Parkinson's disease: recent advances. Curr Opin Neurol 2016; 29: 474–9.

Ungerstedt U, Arbuthnott GW. Quantitative recording of rotational behavior in rats after 6-hydroxy-dopamine lesions of the nigrostriatal dopamine system. Brain Res 1970; 24: 485–93.

Urs NM, Bido S, Peterson SM, Daigle TL, Bass CE, Gainetdinov RR, et al. Targeting beta-arrestin2 in the treatment of L-DOPA-induced dyskinesia in Parkinson's disease. Proc Natl Acad Sci U S A 2015; 112: E2517–26.

Warren Olanow C, Bartus RT, Baumann TL, Factor S, Boulis N, Stacy M, et al. Gene delivery of neurturin to putamen and substantia nigra in Parkinson disease: a double-blind, randomized, controlled trial. Ann Neurol 2015; 78: 248–57.